Decreased Vascular Patterning in the Retinas of Astronaut Crew Members as New Measure of Ocular Damage in Spaceflight-Associated Neuro-ocular Syndrome

Ruchi J. Vyas,[1] Millennia Young,[2] Matthew C. Murray,[3] Marina Predovic,[3] Shiyin Lim,[3] Nicole M. Jacobs,[3] Sara S. Mason,[4] Susana B. Zanello,[5] Giovanni Taibbi,[6] Gianmarco Vizzeri,[6] and Patricia Parsons-Wingerter[7]

[1]SGT Incorporated, NASA Ames Research Center, Mountain View, California, United States
[2]NASA Johnson Space Center, Houston, Texas, United States
[3]Ames Blue Marble Space Institute of Science, NASA Ames Research Center, Mountain View, California, United States
[4]MEI Technologies, NASA Johnson Space Center, Houston, Texas, United States
[5]KBR, NASA Johnson Space Center, Houston, Texas, United States
[6]Department of Ophthalmology and Visual Sciences, The University of Texas Medical Branch at Galveston, Galveston, Texas, United States
[7]Low Gravity Exploration Technology, NASA, Glenn Research Center, Cleveland, Ohio, United States

Correspondence: Patricia Parsons-Wingerter, MS 77-5, NASA Glenn Research Center, Cleveland, OH 44135, USA; patricia.a.parsons-wingerter@nasa.gov.

Received: April 20, 2020
Accepted: November 11, 2020
Published: December 29, 2020

Citation: Vyas RJ, Young M, Murray MC, et al. Decreased vascular patterning in the retinas of astronaut crew members as new measure of ocular damage in spaceflight-associated neuro-ocular syndrome. *Invest Ophthalmol Vis Sci.* 2020;61(14):34. https://doi.org/10.1167/iovs.61.14.34

Purpose. Ocular structural and functional changes, collectively termed spaceflight-associated neuro-ocular syndrome (SANS), have been described in astronauts undergoing long-duration missions in the microgravity environment of the International Space Station. We tested the hypothesis that retinal vascular remodeling, particularly by smaller vessels, mediates the chronic headward fluid shifts associated with SANS.

Methods. As a retrospective study, arterial and venous patterns extracted from 30° infrared Heidelberg Spectralis retinal images of eight crew members acquired before and after six-month missions were analyzed with NASA's recently released VESsel GENeration Analysis (VESGEN) software. Output parameters included the fractal dimension and overall vessel length density that was further classified into large and small vascular branching generations. Vascular results were compared with SANS-associated clinical ocular measures.

Results. Significant postflight decreases in D_f, L_v, and in smaller but not larger vessels were quantified in 11 of 16 retinas for arteries and veins (P value for D_f, L_v, and smaller vessels in all 16 retinas were $\leq$0.033). The greatest vascular decreases occurred in the only retina displaying clinical evidence of SANS by choroidal folds and optic disc edema. In the remaining 15 retinas, decreases in vascular density from D_f and L_v ranged from minimal to high by a custom Subclinical Vascular Pathology Index.

Conclusions. Together with VESGEN, the Subclinical Vascular Pathology Index may represent a new, useful SANS biomarker for advancing the understanding of SANS etiology and developing successful countermeasures for long duration space exploration in microgravity, although further research is required to better characterize retinal microvascular adaptations.

Keywords: SANS, retina, fractal, astronaut, VIIP

Astronauts experience ocular structural and visual impairments when exposed to microgravity on board the International Space Station (ISS), especially during the new long duration missions of six months or more.[1–9] Of variable severity, these changes are denoted collectively by NASA as the spaceflight-associated neuro-ocular syndrome (SANS; previously visual impairments associated with increased intracranial pressure). Risks documented by established clinical methods include optic disc edema (ODE), optic nerve sheath distension, increased total retinal thickness, and choroid thickness, cotton wool spots, and posterior globe flattening with secondary hyperopic shift, accompanied by decreased near visual acuity.[8] Estimations of the incidence of SANS have varied considerably, depending on the clinical measures and cutoff values for SANS. Research on the etiology of this complex syndrome has resulted in several explanations that continue to be actively investigated and focus on the headward fluid shifts incurred in the microgravity environment.[8] After long duration missions, approximately 15% of astronauts have displayed clinically significant (Frisén grade 1–3) ODE, with choroidal folds observed in 20% of astronauts, and subclinical levels of increased ODE, TRT, and choroid thickness documented for the remainder of most crew members.[6,8]

For this study, we tested the hypothesis that blood vessels in the retinas of crew members, particularly the smaller vessels, necessarily remodel to mediate and accommodate the chronic headward fluid shifts believed to be associated with the cardiovascular stresses of prolonged microgravity.[5,6,10,11] A fundamental function of the microvascular endothelium throughout the body is to regulate overall fluid balances within each tissue.[12]

For this investigation, vascular patterns extracted from retinal images of eight astronauts acquired before and after 6-month missions to the ISS were mapped and quantified using NASA's VESsel GENeration Analysis (VESGEN) software.[13–15] Previous research demonstrated the ability of VESGEN to identify oscillatory (alternating), homeostatic-like changes in the vascular patterning of retinas at progressive stages of diabetic retinopathy.[13,16,17] Results for retinas from early to late stages of diabetic retinopathy revealed that vascular remodeling alternated between patterns of increased and decreased vessel density, primarily because of successive alternations between low and high densities of the small vessels. For early in vivo studies on the regulation of angiogenesis and antiangiogenesis by numerous cytokines such as vascular endothelial growth factor (VEGF)-A[18–23] and anti-inflammatory agents,[13,24,25] analysis by VESGEN demonstrated that each molecular regulator induced a unique "fingerprint" or "signature" pattern of vascular response. For example, as a complex cytokine of pluripotent activity, VEGF-A (also termed vascular permeability factor) displayed a phenotypic switch between the stimulation of physiologic angiogenesis at a low concentration to a nonangiogenic pathologic stimulation of vessel dilation and leakage at high concentration.[21] In contrast, basic fibroblast growth factor exerted only a dose-dependent stimulation of robust angiogenesis.[26] The angiogenesis inhibitor angiostatin induced an ill-formed, pathologic response of vascular patterning,[18] whereas the anti-inflammatory clinical steroid triamcinolone acetonide inhibited angiogenesis by not only selectively inhibiting the growth of new small vessels, but also thinning the diameters of all vessels throughout the vascular tree.[24]

The aim of this study was to test whether changes in arterial and venous patterning within crew member retinas during long duration missions offer a useful early-stage predictor, monitor, and new measure of SANS. Based on vascular branching rules such as vessel connectivity and fractal bifurcational branching, the automated vascular mapping and quantification by VESGEN assigns vessels to branching generations for site-specific analysis of changes within complex branching vascular trees.[13] Software output includes informative vascular maps and parameters such as vessel length, diameter, branchpoints and the fractal dimension (D_f). This analytical approach has consistently validated the important role of small vessels in vascular remodeling.[13,17,19,20,24,25,27–29] As developed by Mandelbrot and others,[30,31] fractal geometry describes the complex space-filling patterns observed frequently in nature and in the transport phenomena of physics that include vascular and neuronal branching, arterial river systems, botanical trees, and retinal vascular remodeling.[13,17] As a useful measure of overall vascular space-filling capacity, D_f is of fractional value, unlike the dimensional integers of Euclidean geometry. Branching patterns in human and other vertebrate vascular systems are based to some extent on the fractal property of self-similarity, by which the characteristic vascular bifurcational branching pattern is repeated at decreasing length scales.[31,32]

Table 1. Characteristics of Study Participants (Most Astronauts Were Repeat Flyers)[8]

Sex, *n*	
Male	7
Female	1
Average age, mean (SD)	46.9 (5.4)
Preflight test (days before launch), mean (SD)	144 (100)
Postflight test (days after land), mean (SD)	4.0 (1.7)
Current mission elapsed time (days), mean (SD)	171 (17)
Previous spaceflight experience (days), mean (SD)	11 (15)

Methods

Participants

The retrospective cohort study design of eight U.S. astronaut crew members conformed to the tenets of the Declaration of Helsinki, epidemiological guidelines,[33] and was approved by the Institutional Review Board and Lifetime Surveillance of Astronaut Health (LSAH) at the NASA Johnson Space Center, Houston, Texas, after informed consent by the participants. Because of astronaut privacy rights, only limited and pooled information on characteristics of the study participants is available from LSAH (Table 1). All crew members completed missions of approximately six months aboard the ISS, with preflight and postflight medical exams that included fundoscopy and/or optical coherence tomography (OCT). Crew members were required to meet defined NASA medical standards at crew selection and flight selection, with specific requirements defined for all body systems that include standards for visual/ocular, neurologic, and cardiovascular fitness.[8,34–36] Preflight and postflight exams were performed in the upright position. Exercise prescriptions (especially for resistive exercise) were highly similar for ISS crew members after adjusting for size and gender of the crew member.

Study Design

The study consisted of two phases. First, vascular images of the retinas of eight crew members (de-identified as A–G) acquired preflight and postflight flight by Medical Operations, Johnson Space Center ($n = 8$; 16 retinas; 32 pre/post images) were analyzed with VESGEN by vascular analysts in a blinded manner (i.e., participant identity and pre/post ISS image status were masked to the vascular analysis team). Second, the pre/post status of the images was unmasked to assess vascular changes. Retinal vascular results were compared with ocular and visual measures from clinical findings such as axial length (IOL Master 500, Carl Zeiss Meditec, Dublin, CA), ODE identified during dilated fundus examination from retinal images using a TRC 50EX retinal mydriatic camera (Topcon, Oakland, NJ), and TRT and peripapillary choroidal thickness measured by Heidelberg Spectralis OCT (Heidelberg Engineering GmbH, Heidelberg, Germany).[9]

Image Acquisition and Post Processing

Retinal vascular images (1536 × 1536 pixels^2) acquired by Spectralis infrared (IR) 30° imaging (Heidelberg Engineering) at Medical Operations, Johnson Space Center were centered on the optic disc (average resolution, 6.03 µm/pixel). The track mode of the OCT was used to scan

Table 2. Arterial and Venous Density in 16 Retinas of Eight Crew Members Before and After 6-Month Missions to the ISS.

Vascular Tree	Parameter	Symbol	ISS Status	Results, Mean ± SE	Pre-to-Post Change, Mean ± SE	*P* Value
Arterial	Fractal dimension	D_f	Pre	1.36 ± 0.01		
			Post	1.34 ± 0.01	–0.02 ± 0.007	0.027
	Length density					
	All vessels	L_v	Pre	12.61 ± 0.36		
			Post	11.80 ± 0.27	–0.82 ± 0.37	0.033*
	Large vessels	L_{v1-4}	Pre	7.75 ± 0.31		
			Post	7.85 ± 0.26	–0.10 ± 0.18	0.553
	Small vessels	$L_{v\geq5}$	Pre	4.86 ± 0.45		
			Post	3.95 ± 0.32	–0.92 ± 0.30	0.005
Venous	Fractal dimension	D_f	Pre	1.34 ± 0.01		
			Post	1.33 ± 0.01	0.015 ± 0.005	0.009
	Length density					
	All vessels	L_v	Pre	11.62 ± 0.21		
			Post	10.97 ± 0.29	–0.65 ± 0.38	0.033*
	Large vessels	L_{v1-4}	Pre	5.87 ± 0.25		
			Post	5.98 ± 0.23	+0.010 ± 0.093	0.224
	Small vessels	$L_{v\geq5}$	Pre	5.75 ± 0.30		
			Post	5.00 ± 0.41	–0.75 ± 0.31	0.019

* Both L_v, = 0.033.
L_v, vessel length density. Physical dimensions of L_v, L_{v1-4}, $L_{v\geq5}$, $\times10^{-4}$ µm/µm^2.

Table 3. Case Study of Crew Member A Diagnosed With SANS

Vascular Tree	Parameter	Symbol	ISS Status	Left Retina (no SANS)	Pre-to -Post Change	Right Retina (SANS)	Pre-to -Post Change
Arterial	Fractal dimension	D_f	Pre	1.40		1.40	
			Post	1.39	–0.01	1.33	–0.07
	Length density	L_v	Pre	13.91		13.48	
	All vessels		Post	13.32	–0.59	10.22	–3.25
Venous	Fractal dimension	D_f	Pre	1.36		1.38	
			Post	1.35	–0.01	1.32	–0.06
	Length density	L_v	Pre	11.34		12.11	
	All vessels		Post	11.31	–0.03	9.20	–2.91

L_v, vessel length density. Physical dimensions of L_v, $\times10^{-4}$ µm/µm^2.

the identical retinal area in postflight images from baseline preflight images for exact comparisons of vascular differences. Because the original 1536 × 1536 pixel^2 images were converted during transmission of crew member data to a bitmap (bmp) image format at 496 × 496 pixel,^{2} a scaling factor of 0.3229 was applied to recover the original 1536 × 1536 pixel^2 image resolution for correct calculation of the physical dimensions of parameters for vessel length density.

In brief,[13,17] a binary vascular pattern of overlapping arterial and venous trees was extracted from grayscale IR images by semi-automatic computer processing with Photoshop (Adobe, Mountain View, CA) using large high-resolution Apple monitors (Cupertino, CA). The binary vascular pattern was manually separated into images of arterial and venous trees by comparison with color fundus images (when available) and by basic physiologic principles of vascular tree connectivity, branching, vessel tapering, and arteriovenous pairing. Vessel interpretation was subject to agreement by at least two experienced vascular image analysts (with reviews and final decision by senior analyst).

This report is the first on the application of the VESGEN analysis to a longitudinal study of human retinal images (Tables 1–4). For previous[13,16,17] and concluding studies of diabetic retinopathy, only single images of patients were analyzed as cross-sectional study designs. Consequently, an important new method for this study was the straightforward reconciliation of first the segmented pre/post vascular patterns, and then of the separated arterial and venous trees, described in detail in the Supplementary Data. This process was undertaken to ensure that any differences in the blinded results of the vascular analysis could be attributed to actual differences of vascular response to microgravity, and not to artifacts of the vessel segmentation. Although the quality of the pre/post IR images appeared quite uniform, minor differences in the detection of smaller vessels also probably resulted from inevitable imaging limitations.

Vascular Mapping and Quantification

Each binary arterial or venous image served as the single input image to VESGEN (version 1.0) for automated mapping and quantification (Fig. 1). The software, publicly available with a comprehensive user guide upon request to NASA,[37] is written as a complex plug-in to ImageJ (U.S. National Institutes of Health, Bethesda, MD)[38] and has been validated for the following operating systems: Microsoft Windows and MacOS through Mojave (Catalina is currently being tested). Output calculated by the software includes various arterial and venous maps, D_f and L_v that is further divided into specific branching generations G_1, G_2,…G_6 as L_{v1-4} and $L_{v\geq5}$

Investigative Ophthalmology & Visual Science

Table 4. SVPI for SANS From Preflight to Postflight Changes

Status	Rank	ID	Eye	D_f Scale (%)	L_v(all) Scale (%)	Overall Scale (%)	SVPI Index
SANS clinical index	1	A	OD	100	100	100	–
Subclinical index	1	B	OS	83	69	76	Highest
	2	B	OD	75	75	75	
	3	C	OS	67	67	67	
	4	E	OD	33	36	35	
	5	D	OD	33	32	33	
	6	D	OS	25	21	23	
	7	A	OS	17	10	14	
	8	H	OD	42	–18	12	
	9	F	OS	8	13	11	
	10	E	OS	8	7	8	Lowest
	0	F	OD	0	–2	–1	No vascular decrease
	0	C	OD	0	–8	–4	
	0	H	OS	–8	–8	–8	
	0	G	OS	–17	–7	–12	
	0	G	OD	–25	–25	–25	

L_v, vessel length density; OD, right eye; OS, left eye. For deidentified crew members (A–G), a relative scale of change in D_f and L_v averaged from arteries and veins was calculated for each left (OS) and right (OD) retina from the ratio of pre-to-post change normalized to the SANS retina. Values were then averaged for the overall scale to determine subclinical ranking. (A, only retina diagnosed with SANS.)

(Fig. 1).[13] For a two-dimensional binary image, D_f varies as a fractional value between 1 and 2 and for skeletonized vascular images, typically from 1.22 to 1.48. As further examples, L_{v1-4} denotes L_v with respect to branching generations G_1 to G_4 (Fig. 1). Physical dimensions such as L_v = 0.000775 µm/µm^2 are notated as 7.75 × 10^{-4} µm/µm^2. The terms "vascular increase" and "vascular decrease" are used to summarize the increase or decrease in vascular density as measured by D_f, L_v, L_{v1-4}, and $L_{v\geq5}$.

Relative decreases in vessel diameter and other considerations of vessel branching and tapering are used to classify the vessel branching generations (G_1–G_x), based on previous experimental results for heart and lung vascular branching[39–41] and the conservation of laminar blood flow.[10] At a symmetric vessel bifurcation, the diameter of the offspring vessels decreases to 71% ($1/\sqrt{2}$) of the diameter of the parent vessel. The averaged decrease in vessel diameter to 71%, together with an (adjustable) tolerance factor of ±15% that accounts for the realistic asymmetry of biological vascular branching (Fig. 1), is used by VESGEN as the primary determinant of a new branching generation.

Statistics

Analyses were conducted using linear mixed models that included subject-specific random effects to account for repeated measures of the left and right eyes within individuals. Primary VESGEN measures included D_f, L_v, L_{v1-4}, and $L_{v\geq5}$ measured for each vascular tree (arteries or veins). Time (pre or post) was included as a categorical fixed effect. Models were fit in SAS v9.4 using PROC GLIMMIX. The LSMEANS and LSMESTIMATE statements were used to estimate means and standard errors of the time-specific response and the premission to postmission change in VESGEN measures (threshold for confidence, $P < 0.05$). Additional models included axial length as a covariate to assess the association with VESGEN parameters.

Changes in the VESGEN parameters were compared with the axial length as described elsewhere in this article and observationally compared with a fundoscopic diagnosis of ODE, changes in axial length, and changes in TRT and peripapillary choroidal thickness. There was only one instance of fundoscopy-identified ODE, leading to a minimal statistical resolution of $P = 0.0625$ (1/16). All possible permutations of the one diagnosis of ODE by fundoscopy compared with the other 15 retinas were used to estimate an empirical P value for the association. Because this single ODE was identified in the retina that also had the largest vascular changes measured by VESGEN, the empirical P value matched the minimal resolution ($P = 0.0625$). Change in TRT is considered as one of the earliest signs of the development of ODE. Unfortunately, premission to postmission TRT change measures were not available for two of the three subjects (four retinas) displaying the largest changes in vascular parameters, as well as for axial length and peripapillary choroidal thickness in several subjects. Therefore, the association between changes in VESGEN parameters and TRT, axial length and peripapillary choroidal thickness could only be reported individually.

Results

Summary of Approach

The study comprised 32 preflight and postflight images collected by the Heidelberg OCT 30° IR mode from the two eyes of eight crew members. Post-ISS changes in overall arterial and venous patterning were quantified by D_f and L_v. In addition, length densities of large and small vessels by L_{v1-4} and $L_{v\geq5}$ were calculated for branching generations of G_{v1-4} and $G_{v\geq5}$. Results are reported as (1) post-ISS trends of vascular patterning in the retinas of all crew members, (2) vascular response in the retinas of individual crew members, (3) association of trends in vascular patterning with clinical ocular measures, and (4) a subclinical vascular pathology index (SVPI) calculated from clinical incidence of SANS.

Post-ISS Trends of Vascular Patterning in Retinas of All Crew Members

The overall vascular space-filling capacity by D_f decreased in both arterial and venous trees after 6 months in microgravity, when averaged for all 16 crew member retinas (from Table 2,

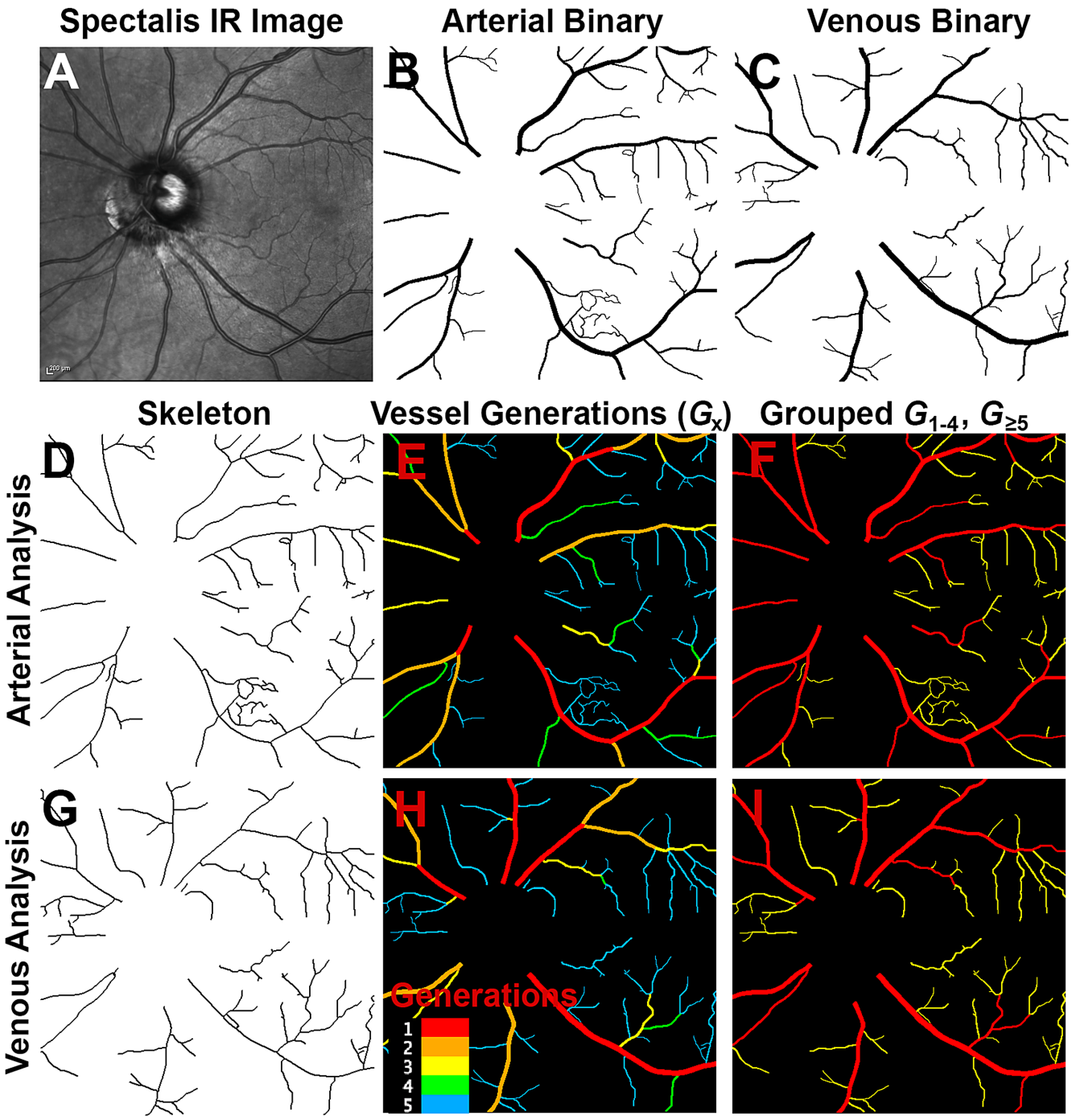

Figure 1. Mapping and quantification of vascular branching trees. Binary images of arterial and venous trees extracted from the grayscale Spectralis IR image of the left retina of astronaut crew member E acquired before a 6-month mission to the ISS (**A–C**) served as sole inputs for the vascular maps (**D–I**). Specialized algorithms in VESGEN first calculate a skeleton (*centerline*) of the trees (**D**, **G**) that together with the input binary image generate further mappings such as the branching generations maps (**E**, **H**).[13] The arterial and venous branching generations denoted in the legend were grouped by the software into large (*red*, L_{v1-4}) and small (*yellow*, $L_{v\geq 5}$) vessels using a VESGEN user-interactive option (**F**, **I**). This retina experienced the lowest vascular decrease of the 11 retinas for which postflight vascular decreases were measured. By VESGEN quantification of these and other vascular maps, arterial and venous D_f are 1.354 and 1.329, and overall arterial and venous length densities (L_v), 12.1 × 10^{-4} µm/µm^2 and 10.7 × 10^{-4} µm/µm^2. For the postflight image, arterial and venous D_f are 1.349 and 1.343, and overall arterial and venous length densities (L_v), 11.88 × 10^{-4} µm/µm^2 and 11.37 × 10^{-4} µm/µm^2.

arterial mean change in D_f, –0.02; SE, 0.006; P = 0.027; and venous mean change; –0.015; SE, 0.005; P = 0.009; see also Supplementary Table S1). As predicted, the length density of larger vessels in the first four branching generations, L_{v1-4}, was relatively unchanged. However, significant decreases were measured in $L_{v\geq 5}$ (arterial mean change, –0.92; SE, 0.30; P = 0.005; and venous mean change, –0.75; SE, 0.31; P = 0.019). Results indicate that vascular adaptations

to microgravity occurred primarily in the smaller vessels. In general, decreases in the density of these smaller vessels were greater for small arteries than for small veins. As indicated by the low variability, D_f is a sensitive measure of change in vascular space-filling capacity, although absolute numerical changes in D_f are not large (Table 1, Supplementary Table S1).[16,18–21,24]

Vascular Response in Retinas of Individual Crew Members

Of the eight crew members, only the right eye of crew member A was diagnosed by NASA with SANS. Abnormal, degenerative postflight changes by several clinical measures established for SANS by NASA included the largest increase in TRT, ODE, and choroidal folds by fundoscopy imaging (Fig. 2). This retina displayed the largest decreases in both arterial and venous space-filling density by D_f and L_v (Tables 2, 3, 4, and Supplementary Table S1). Postflight decreases in the patterning of small vessels by $L_{v\geq5}$ (yellow vessels, Fig. 2, J, R) are apparent by visual inspection in comparison with the preflight retina (yellow vessels, Fig. 2, I, Q). In contrast, arterial and venous patterning within the left retina of crew member A remained relatively unchanged (Tables 2, 3, and Supplementary Table S1, Fig. 2).

The largest vascular decreases associated with subclinical results for SANS by fundoscopy examination occurred bilaterally in the retinas of crew member B (Table 4, Fig. 3). Overall, postflight vascular density decreased in 11 of 16 retinas by more than 0.02, a cutoff value for D_f estimated from previous studies in which changes greater than 0.02 or 0.03 were meaningful for distinguishing between sampling or treatment groups (Supplementary Table S1).[16,18–21,24]

Association of Trends in Vascular Patterning with Clinical Ocular Measures for SANS and Other Ocular Response

Results from data visualization (Fig. 4) and permutation testing of the eight subjects indicate that vascular decreases in D_f, L_v, and $L_{v\geq5}$ appear to be positively associated with pre/post mission incidence of clinical measures that include ODE, choroidal folds identified through fundoscopy (by permutation testing, $P = 0.0625$), pre/post mission decreases in axial length, increased TRT, and, to some extent, increased peripapillary choroidal thickness. Measurements of TRT were lacking for two of the three crew members with the largest vascular pre/post vascular decreases, and of axial length and peripapillary choroidal thickness in a number of crew members. It is not known whether those retinas lacking TRT data experienced changes larger than the increase of 19.4 µm in TRT that recently is now viewed by NASA as the earliest signs of ODE leading to SANS.

None of the participants reported visual changes. Subject A, who displayed the largest decrease in vascular density (Table 4), the largest ODE by OCT and fundoscopy, and the greatest change in globe flattening and refractive error (0.75 diopters), was also a myope, which may account for the lack of functional impact. Hyperopic refractive error shifts are the primary characteristics of functional change with spaceflight.[8] By regression analysis, a greater axial length was associated with greater arterial and venous density by the space-filling measure of D_f and density of smaller vessels ($L_{v\geq5}$), but decreased the density of larger vessels (L_{v1-4}), whether in the preflight or postflight globe ($n = 14$; Table 5). When included in the mixed models as a covariate, Table 5 outlines the coefficient estimates and P values.

SVPI From the Clinical Incidence of SANS

To further examine postflight trends in decreased arterial and venous patterning, results from the VESGEN analysis within individual retinas were ranked from one to 16 by the SVPI according to greatest vascular loss for estimation of potential subclinical vascular pathology and risk for SANS. Briefly, magnitudes of arterial and venous changes by D_f and L_v for each of the 15 retinas found to be clinically normal by fundoscopy were averaged and compared with changes in the right retina of crew member A as the SANS reference value (i.e., normalized to the SANS retina; Table 4). Negative values by SVPI indicate a postflight increase in vascular density. By the SVPI, 10 retinas experienced pre/post vascular decreases from 8% to 76% of the decrease in the SANS retina. The largest subclinical vascular decreases occurred bilaterally in the retinas of crew member B (Fig. 3). Smaller postflight decreases in vascular density within some retinas may indicate a vascular-protective adaptation against SANS ocular structural changes. Alternatively, these 10 retinas may represent varying levels of early stage subclinical microvascular injury incurred during prolonged microgravity.

Retinas of five crew members with slight increases in vascular density from 2% to 15% were rendered in the SVPI as negative values (i.e., as gains in vascular density added to the total scale of vascular decrease from 0% to 100% established by the SANS retina). Vascular changes from –25% to +25% may represent the level of measurement error (background) in the IR images resulting from the limiting vascular resolution of Spectralis imaging.

Discussion

After six months on the ISS, 70% of astronaut retinas (11/16) exhibited microvascular decreases by VESGEN vascular analysis (i.e., decreases in $L_{v\geq5}$). Overall decreases in arterial and venous densities, and decreases in small but not large vessels, provide preliminary confirmation of the hypothesis that blood vessels in the retina, particularly the smaller vessels, remodel to accommodate the prolonged fluid shifts experienced in microgravity. A further important result is that the loss of vessel density appeared to be similar for both arteries and veins.

To our knowledge, this report is the first on the decrease of retinal vascular patterning in response to long-duration microgravity. The trend toward vascular decrease, particularly of the small vessels, was confirmed by several approaches that include (1) statistical analysis of premission to postmission changes by several confirming measures (D_f, L_v, and $L_{v\geq5}$; all $P \leq 0.033$); (2) association of greatest vascular loss with the one retina diagnosed with SANS from ODE and choroidal folds by fundoscopy; and greatest changes in TRT by OCT (from permutation testing; $P = 0.0625$) and axial length (but not with increased peripapillary thickness); (3) observational association of the range of vascular decrease in the 16 retinas with TRT, and (4) calculation of the range of subclinical vascular loss (SVPI) in 15 retinas compared with the maximal loss in the single SANS retina. Vascular decreases determined by this study ranged from none to considerable, as could be predicted

Investigative Ophthalmology & Visual Science

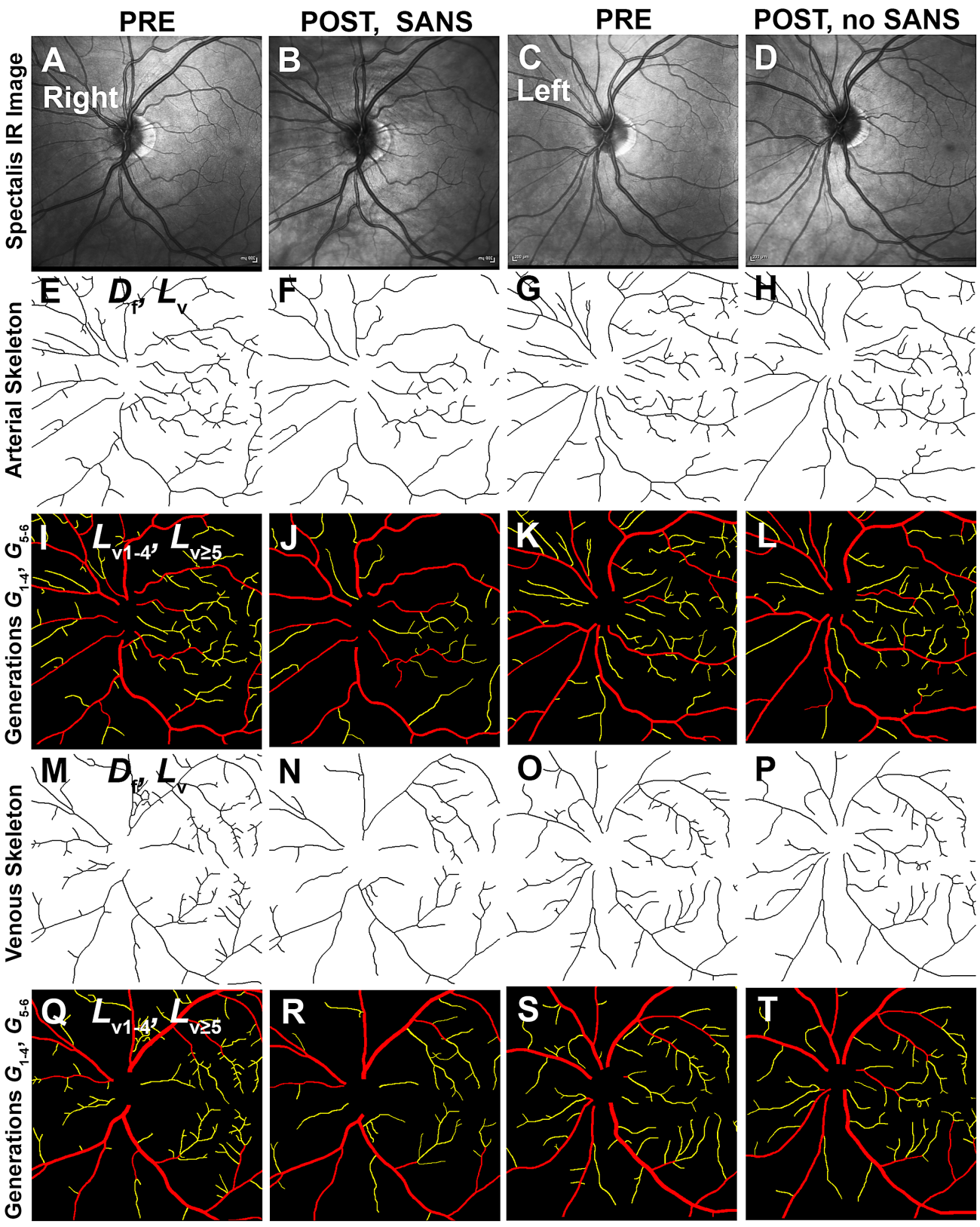

Figure 2. Decreased vascular patterning in the right retina of ISS crew member A diagnosed with SANS. Arterial and venous postflight decreases in the right retina, but not left retina, are clearly visible in several vascular maps. The right retina was the only retina in this cohort diagnosed with SANS by fundoscopy examination from ODE and choroidal folds, visible in the postflight image at higher zoom. Binary vascular trees extracted from Spectralis IR grayscale images of the (**A**, **B**) right and (**C**, **D**) left retinas were automatically analyzed by the VESGEN software as (**E–H**, **M–P**) vascular skeletons and (**I–L**, **Q–T**) vessel branching grouped into large (G_{v1-4}, *red*) and small (G_{v5-6}, *yellow*) generations. The arterial and venous D_f and overall length densities (L_v) for this crew member are reported as an individual case study in Table 3. For visual comparison of vascular patterns, all images were aligned with optic nerve to left (image of right retina rotated 180°).

Investigative Ophthalmology & Visual Science

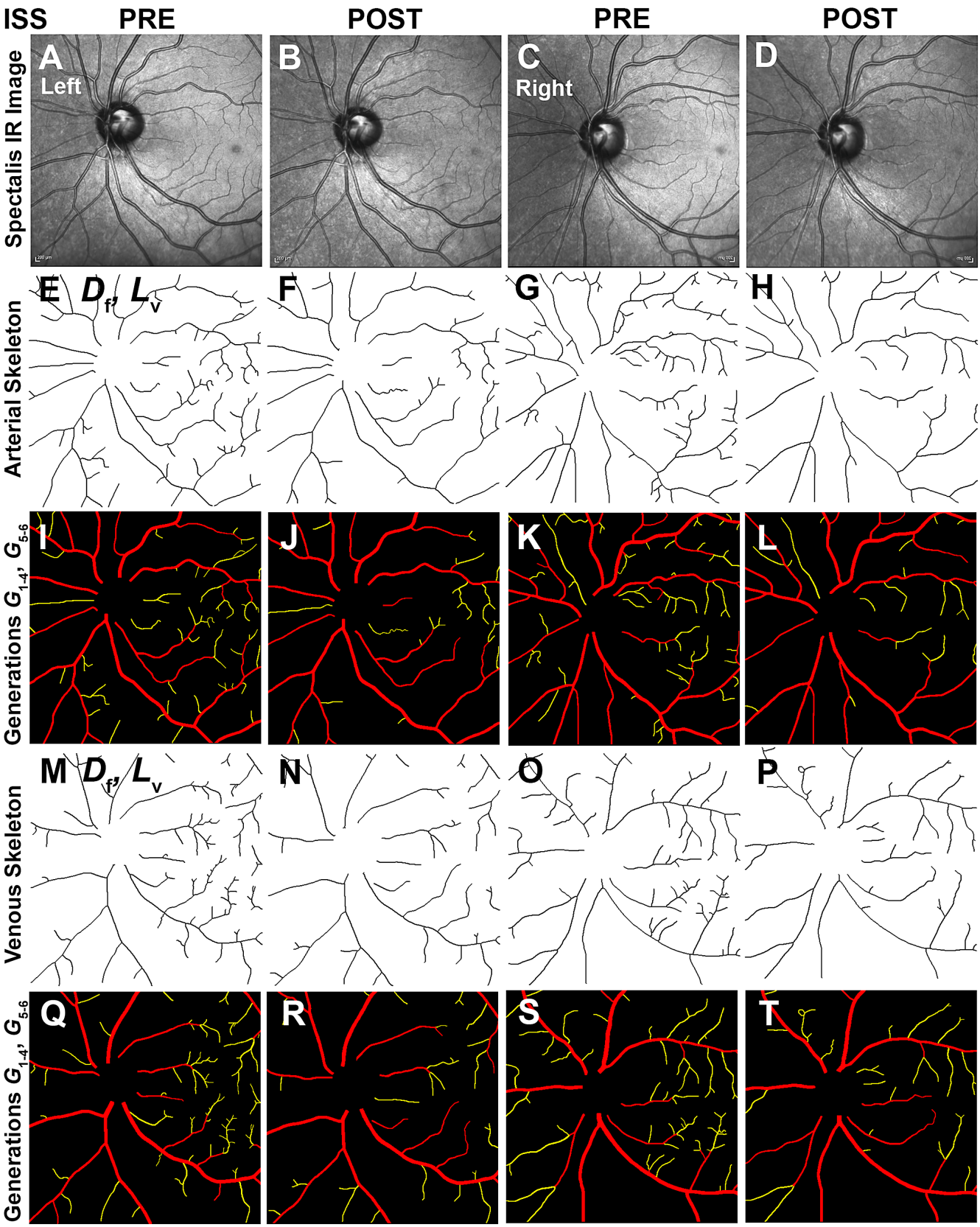

Figure 3. Vascular decrease in the retinas of crew member B after 6 months on the ISS. Arterial and venous density decreased in the postflight left and right retinas to 76% and 75%, compared with a scale of 100% loss in the right retina of crew member A (Fig. 2, Table 4). As for crew member A, binary arterial and venous trees extracted from grayscale images of the left and right retinas (**A–D**) were analyzed by VESGEN as vascular skeletons (**E–H**, **M–P**) and generational branching grouped into large (G_{v1-4}, *red*) and small (G_{v5-6}, *yellow*) generations (**I–L**, **Q–T**).

Investigative Ophthalmology & Visual Science

Table 5. Positive Association of Postflight Increases in Axial Length (per mm) of Ocular Globes With Postflight Change in Vascular Parameters

Vessels	Parameter	Coefficient	SE	*P* Value
Arteries	Df	0.014	0.004	0.01
	Lv5+	0.0003	0.00008	0.003
	Lv1-4	−0.0001	0.00006	0.03
Veins	Df	0.011	0.004	0.01
	Lv5+	0.0002	0.00007	0.02
	Lv1-4	−0.00005	0.00005	0.32

L_v, vessel length density. Physical dimensions of L_v, $\times 10^{-4}$ μm/μm^2. By covariate regression analysis of mixed models (n = 14, Fig. 4). Overall by mean ± SE [minimum, maximum], postflight axial length increased from preflight axial length, 24.33 ± 0.28 mm [23.72, 24.95] to 24.21 ± 0.27 mm [23.64, 24.79].

from the variable incidence reported for SANS.[1–3,5,6,8] Significant decreases in vascular density occurred both unilaterally and bilaterally, as reported previously for other ocular measures associated with SANS.[1,2]

Results of this investigation suggest that vascular patterning may offer an early stage predictor and biomarker of future susceptibility to SANS ocular structural changes. Further investigations on the role of the microvasculature in the retina are important for a more complete understanding of SANS etiology and the development of successful countermeasures. Results demonstrate that the VESGEN analysis, if validated by future studies on early stage detection of vascular loss, could potentially be adapted for flight monitoring of SANS susceptibility using ISS OCT data.

Investigations on SANS by other approaches propose potential causes resulting in fluid changes within the eye[5,6,10,42] that may be multifactorial, such as systemic cardiovascular disturbances, increased intracranial pressure and structural changes in the brain leading to transduction of fluid through the optic nerve to the eye,[43–46] and nutritional, hypercapnic, genetic, and inflammatory status.[6,43,44,47–49] From terrestrial measurements of sequential peripapillary TRT measures within the same subjects across multiple days, in multiple postures and with multiple analysts, a change of 19.4 μm was determined to have less than a 5% chance of being due to these sources of measurement variability, offering a potential cutoff value for the earliest sign of ODE. As reported recently, an increased IOP has not been shown to be strongly associated with SANS, and IOP normalizes to preflight values after 4 days of spaceflight.[50]

Crucial to the understanding of how these vascular decreases influence the development of SANS during long duration microgravity is whether the small vessels underwent vaso-obliteration (vessel dropout or loss), or the diameters of small vessels in the retina simply decreased below the limit of image resolution, or both. We speculate that the vascular decreases most likely resulted from decreased vessel diameter (caliber). Potential etiologic mechanisms of decreased vessel diameter include systemic losses in blood volume as reported previously.[42,51] Spaceflight hypovolemia of approximately 10% is ascribed to several causes that include reduced fluid intake, loss of erythrocytes, and potentially faster fluid shifts from intravascular to interstitial spaces, resulting from lower transmural pressures because of decreased compression of tissues in microgravity, especially within the thorax.[42,51] Alternatively, vascular decreases may be secondary to vascular compression from optic disc/peripapillary swelling.[52–54]

Edematous fluid transfers by sources such as an increased intracranial pressure and ODE, in addition to the globe flattening reported here and in many other previous studies, may cause high extravascular fluid pressures within the eye to constrict vessels and impede blood flow, perhaps to the level of vessel dropout. Such extravascular tissue pressure may be analogous to the "compartment syndrome" described for injuries such as tibial fracture, abdominal organ failure, or surgery, in which tissue injury accompanied by excessive edema overcomes the ability of the microvascular endothelium to mediate the disturbed fluid balances, resulting in tissue damage or necrosis.[52–54] Or retinal and ODEs may have obscured the vessels, which implies that changes reported here may in part or fully derive from vessel obscuration.

New studies with higher resolution ophthalmic imaging such as Spectralis IR of unmodified resolution (see Methods) or OCT angiography are clearly necessary to determine whether these vascular changes are due to decreased vessel diameter, vaso-obliteration, vessel obscuration, or a combination of these factors. Although the diameters of smaller vessels may have decreased in microgravity, the diameters of larger vessels did not appear to change significantly (data not included because of limitations in the relatively low-resolution Spectralis IR vascular imaging for reliable determination of vessel diameter). Unsurprisingly, given the level of Spectralis IR resolution of 6.03 μm/pixel, the diameters of the smallest vessels detected in all images for our study were slightly less than 12 μm, or two pixels. Thus, postflight decreases in vessel diameter below this imaging cutoff value would not be detectable by the analysis.

For now, we can only speculate on the significance of the negative values in the SVPI of 25% or less. Such negative values may represent a positive retinal vascular adaptation to long-duration microgravity that helps to accommodate the excess headward fluid shifts. An alternative, perhaps more plausible, explanation is that ±25% values of vascular change may represent the current level of noise in the VESGEN analysis. The limited resolution of OCT Spectralis IR vascular imaging mode, unlike that of OCT angiography or fluorescein angiography, is not optimal for the sensitive detection of smaller blood vessels. However, Spectralis IR was the only vascular imaging mode available for our study. It is possible but unlikely that postflight decreases in axial length altered the fidelity of OCT tracking for reproducible imaging of retinal vessels.

The analysis of vascular patterning in the astronaut retina is the first longitudinal study of human subjects using the VESGEN software, following previous cross-sectional studies of diabetic retinopathy as a technology proof of principle.[10,13,14] Limitations of this study include the small number of subjects and relatively low resolution of the vascular imaging by the modified Spectralis IR (see Methods). Currently, Spectralis IR is the only retinal vascular imaging available to NASA Medical Operations before, during, and after ISS missions. The quality of the scanning acquisition for all images appeared highly similar but not identical, differing only slightly in image sharpness, contrast, and retinal field of view. Despite these limitations, the pre/post mission results reveal a clear trend of vascular decrease for this cohort. In previous studies with VESGEN on other applications,[13,16–25,28,29] the significance of vascular trends was also of relatively strong statistical significance, perhaps because hundreds of vessels are captured in a typical clinical or microscopic microvascular image.

Investigative Ophthalmology & Visual Science

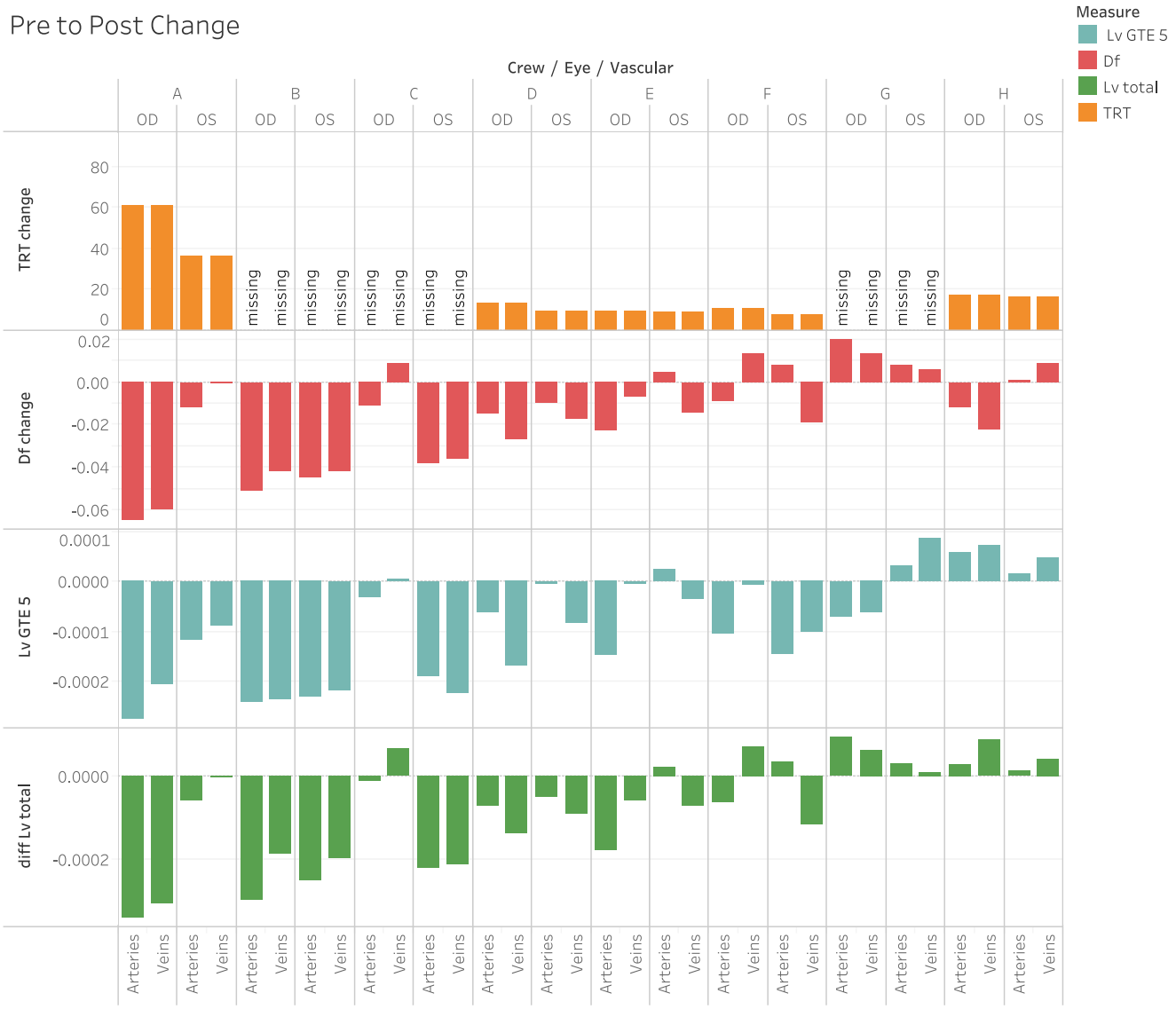

Figure 4. Comparison of pre-to-post flight change in clinical ocular measures with D_f, L_v, and $L_{v\geq5}$. Subjects are ordered by increasing postmission decrease in D_f. The largest increase in TRT and axial length, but not peripapillary choroidal thickness, occurred in the right retina of crew member A diagnosed with SANS by ODE and choroidal folds from fundoscopy examination.

Larger ocular globes were found to be positively associated with the increased density of small vessels and decreased density of large arteries. The decreased density of large, major arborizing vessels in larger eyes is understandable, as this vascular patterning is relatively fixed and constant among all eyes. The increased density of smaller vessels probably arises from the limiting Spectralis IR image resolution. Small vessels are perhaps proportionally larger in larger eyes and therefore more detectable at limits of resolution. Despite this methodological limitation, the vascular analysis nonetheless detected the trend toward postflight decreases in vascular patterning with strong statistical significance.

New segmentation methods are being developed at NASA for the automated extraction of vascular pattern based on artificial intelligence and machine learning algorithms (VESGEN v1.11, scheduled for global release in 2020–2021).[37] In addition to the vascular maps and parameters reported here (D_f and L_v), additional output calculated by the software includes other vascular maps and options for vascular network analysis, vessel tortuosity, vessel diameter, and densities of vessel number, vessel area, and vessel branch point specified for branching generations G_1, G_2,…G_x.[13]

In conclusion, the results of this proof-of-concept investigation show that vascular density decreased in the astronaut retinas after six-month missions to the ISS in microgravity. Vascular patterning may offer a valuable early stage predictor, ongoing monitor, and new diagnostic of retinal status for SANS, a high-priority risk defined by NASA for long duration space exploration missions such as Mars. From extensive international research on the ISS habitat, we are beginning to understand the significance of factors such as microgravity, hypobaria, hypoxia, and hypercapnia for future habitats of long-duration space exploration. Yet much remains to be learned. The effect of partial lunar gravity on vascular adaptations in the retina, for example, is not yet known.

Investigative Ophthalmology & Visual Science

Acknowledgments

Supported by the National Aeronautics and Space Administration (NASA) with Grant NNJ12ZSA002N by the Human Research Program (HRP) and additional support by the HRP Space Radiation and Vascular Centennial Challenge Programs to P.P.W. We thank Robert Ploutz-Snyder, University of Michigan, for initial biostatistical and power analysis design of the study, and Peter Norsk (HRP, NASA) for suggesting the SVPI.

Disclosure: **R.J. Vyas,** None; **M. Young,** None; **M.C. Murray,** None; **M. Predovic,** None; **S. Lim,** None; **N.M. Jacobs**, None; **S.S. Mason,** None; **S.B. Zanello,** None; **G. Taibbi,** None; **G. Vizzeri,** None; **P. Parsons-Wingerter,** None

References

1. Mader TH, Gibson CR, Pass AF, et al. Optic disc edema, globe flattening, choroidal folds, and hyperopic shifts observed in astronauts after long-duration space flight. *Ophthalmology*. 2011;118:2058–2069.
2. Lee AG, Mader TH, Gibson CR, Tarver W. Space flight-associated neuro-ocular syndrome. *JAMA Ophthalmol*. 2017;135:992–994.
3. Lee SMC, Stenger MB, Laurie SS, Macias BR. *Evidence report: risk of cardiac rhythm problems during spaceflight*. U.S. National Aeronautics and Space Administration. 2017. Available at: https://humanresearchroadmapnasagov/evidence/reports/Arrhythmiapdf. Accessed June 10, 2020.
4. Patel N, Pass A, Mason S, Gibson CR, Otto C. Optical coherence tomography analysis of the optic nerve head and surrounding structures in long-duration International Space Station astronauts. *JAMA Ophthalmol*. 2018;136:193–200.
5. Zhang LF, Hargens AR. Spaceflight-induced intracranial hypertension and visual impairment: pathophysiology and countermeasures. *Physiol Rev*. 2018;98:59–87.
6. Marshall-Goebel K, Laurie SS, Alferova IV, et al. Assessment of jugular venous blood flow stasis and thrombosis during spaceflight. *JAMA Network Open*. 2019;2:e1915011.
7. Laurie SS, Lee SMC, Macias BR, et al. Optic disc edema and choroidal engorgement in astronauts during spaceflight and individuals exposed to bed rest. *JAMA Ophthalmol*. 2020;138:165–172.
8. Lee AG, Mader TH, Gibson CR, et. Spaceflight associated neuro-ocular syndrome (SANS) and the neuro-ophthalmologic effects of microgravity: a review and an update. *NPJ Microgravity*. 2020;6:7.
9. Macias BR, Patel NB, Gibson CR, et al. Association of long-duration spaceflight with anterior and posterior ocular structure changes in astronauts and their recovery. *JAMA Ophthalmol*. 2020;138:553–559.
10. Hargens AR, Richardson S. Cardiovascular adaptations, fluid shifts, and countermeasures related to space flight. *Respir Physiol Neurobiol*. 2009;169(suppl 1):S30–S33.
11. Nelson ES, Mulugeta L, Myers JG. Microgravity-induced fluid shift and ophthalmic changes. *Life (Basel)*. 2014;4:621–665.
12. Hall JE. *Guyton and Hall Textbook of Medical Physiology*. 13th ed. Philadelphia: Elsevier; 2016.
13. Vickerman MB, Keith PA, McKay TL, et al. VESGEN 2D: automated, user-interactive software for quantification and mapping of angiogenic and lymphangiogenic trees and networks. *Anat Rec*. 2009;292:320–332.
14. HERO Solicitation 80JSCC019N001. U.S. National Aeronautics and Space Administration. Available at: https://nspires.nasaprs.com/external/solicitations/summary.do?method=init&solId={ECBA3DAC-FFA3-F564-D56D-452F818EE1EA}&path=closedPast. Accessed 2019.
15. Parsons-Wingerter P, Vickerman MB. Bioinformatic analysis of vascular patterning. *U.S. Patent. 10,282,841, 2019*.
16. Avakian A, Kalina RE, Sage EH, et al. Fractal analysis of region-based vascular change in the normal and non-proliferative diabetic retina. *Curr Eye Res*. 2002;24:274–280.
17. Parsons-Wingerter P, Radhakrishnan K, Vickerman MB, Kaiser PK. Oscillation of angiogenesis with vascular dropout in diabetic retinopathy by VESsel GENeration analysis (VESGEN). *Invest Ophthalmol Vis Sci*. 2010;51:498–507.
18. Parsons-Wingerter P, Lwai B, Yang MC, et al. A novel assay of angiogenesis in the quail chorioallantoic membrane: stimulation by bFGF and inhibition by angiostatin according to fractal dimension and grid intersection. *Microvasc Res*. 1998;55:201–214.
19. Parsons-Wingerter P, Elliott KE, Farr AG, Radhakrishnan K, Clark JI, Sage EH. Generational analysis reveals that TGF-beta1 inhibits the rate of angiogenesis in vivo by selective decrease in the number of new vessels. *Microvasc Res*. 2000;59:221–232.
20. Parsons-Wingerter P, Elliott KE, Clark JI, Farr AG. Fibroblast growth factor-2 selectively stimulates angiogenesis of small vessels in arterial tree. *Arterioscler Thromb Vasc Biol*. 2000;20:1250–1256.
21. Parsons-Wingerter P, Chandrasekharan UM, McKay TL, et al. A VEGF165-induced phenotypic switch from increased vessel density to increased vessel diameter and increased endothelial NOS activity. *Microvasc Res*. 2006;72:91–100.
22. Parsons-Wingerter P, McKay TL, Leontiev D, Vickerman MB, Condrich TK, Dicorleto PE. Lymphangiogenesis by blinded vessel sprouting is concurrent with hemangiogenesis by vascular splitting. *Anat Rec*. 2006;288:233–247.
23. Liu H, Yang Q, Radhakrishnan K, et al. Role of VEGF and tissue hypoxia in patterning of neural and vascular cells recruited to the embryonic heart. *Dev Dyn*. 2009;238:2760–2769.
24. McKay TL, Gedeon DJ, Vickerman MB, et al. Selective inhibition of angiogenesis in small blood vessels and decrease in vessel diameter throughout the vascular tree by triamcinolone acetonide. *Invest Ophthalmol Vis Sci*. 2008;49:1184–1190.
25. Chen X, Yang G, Song JH, et al. Probiotic yeast inhibits VEGFR signaling and angiogenesis in intestinal inflammation. *PloS One*. 2013;8:e64227.
26. Parsons-Wingerter P, Elliott KE, Clark JI, Farr AG. Fibroblast growth factor-2 selectively stimulates angiogenesis of small vessels in arterial tree. *Arterioscler Thromb Vasc Biol*. 2000;20:1250–1256.
27. Parsons-Wingerter P, Chandrasekharan UM, McKay TL, et al. A VEGF165-induced phenotypic switch from increased vessel density to increased vessel diameter and increased endothelial NOS activity. *Microvasc Res*. 2006;72:91–100.
28. Parsons-Wingerter P, Reinecker HC. For application to human spaceflight and ISS experiments: VESGEN mapping of microvascular network remodeling during intestinal inflammation. *Grav Space Biology*. 2012;26:2–12.
29. Zamanian-Daryoush M, Lindner D, Tallant TC, et al. The cardioprotective protein apolipoprotein A1 promotes potent anti-tumorigenic effects. *J Biol Chem*. 2013;288:21237–21252.
30. Mandelbrot BB. *The Fractal Geometry of Nature*. San Francisco: W. H. Freeman; 1983.
31. Bassingthwaighte JB, Liebovitch LS, West BJ. *Fractal Physiology*. New York: Oxford University Press; 1994.
32. Schwen LO, Preusser T. Analysis and algorithmic generation of hepatic vascular systems. *Int J Hepatol*. 2012;2012:357687.

33. Cuschieri S. The STROBE guidelines. *Saudi J Anaesth*. 2019;13:S31–S34.
34. Barratt MR, Baker E, Pool E. *Principles of Clinical Medicine for Space Flight*. 2nd ed. New York: Springer-Verlag; 2019.
35. Eye Examinations. Medical Requirements Overview12/11/17. U.S. National Aeronautics and Space Administration. Available from: https://lsda.jsc.nasa.gov/lsda_data/document/Project/MRID/MEDB_1.10_1.10.1_Eye%20Examinations%2012_11_17_Project_13_27_17.pdf.
36. U.S. National Aeronautics and Space Administration. Medical operations. Available at: https://lsda.jsc.nasa.gov/MRID. Accessed June 10, 2020.
37. https://software.nasa.gov/software/ARC-17621-1: Vessel Generation Analysis (VESGEN) 2D Software. Publicly released. February 2019. U.S. National Aeronautics and Space Administration.
38. https://imagej.nih.gov/ij/download.html: ImageJ. U.S. National Institutes of Health.
39. Gan RZ, Tian Y, Yen RT, Kassab GS. Morphometry of the dog pulmonary venous tree. *J Appl Physiol*. 1993;75:432–440.
40. Kassab GS, Rider CA, Tang NJ, Fung YC. Morphometry of pig coronary arterial trees. *Am J Physiol*. 1993;265:H350–H365.
41. Kassab GS, Lin DH, Fung YC. Morphometry of pig coronary venous system. *Am J Physiol*. 1994;267:H2100–H2113.
42. Norsk P, Asmar A, Damgaard M, Christensen NJ. Fluid shifts, vasodilatation and ambulatory blood pressure reduction during long duration spaceflight. *J Physiol*. 2015;593:573–584.
43. Koppelmans V, Bloomberg JJ, De Dios YE, et al. Brain plasticity and sensorimotor deterioration as a function of 70 days head down tilt bed rest. *PloS One*. 2017;12:e0182236.
44. Roberts DR, Albrecht MH, Collins HR, et al. Effects of spaceflight on astronaut brain structure as indicated on MRI. *N Engl J Med*. 2017;377:1746–1753.
45. Marshall-Goebel K, Damani R, Bershad EM. Brain physiological response and adaptation during spaceflight. *Neurosurgery*. 2019;85:E815–E821.
46. Riascos RF, Kamali A, Hakimelahi R, et al. Longitudinal analysis of quantitative brain MRI in astronauts following microgravity exposure. *J Neuroimaging*. 2019;29:323–330.
47. Smith SM, Zwart SR. Spaceflight-related ocular changes: the potential role of genetics, and the potential of B vitamins as a countermeasure. *Curr Opin Clin Nutr Metab Care*. 2018;21:481–488.
48. Zanello SB, Tadigotla V, Hurley J, et al. Inflammatory gene expression signatures in idiopathic intracranial hypertension: possible implications in microgravity-induced ICP elevation. *NPJ Microgravity*. 2018;4:1.
49. Zwart SR, Laurie SS, Chen JJ, et al. Association of genetics and B vitamin status with the magnitude of optic disc edema during 30-day strict head-down tilt bed rest. *JAMA Ophthalmol*. 2019;137:1195–1200.
50. Huang AS, Stenger MB, Macias BR. Gravitational influence on intraocular pressure: implications for spaceflight and disease. *J Glaucoma*. 2019;28:756–764.
51. Diedrich A, Paranjape SY, Robertson D. Plasma and blood volume in space. *Am J Med Sci*. 2007;334:80–85.
52. McQueen MM, Christie J, Court-Brown CM. Acute compartment syndrome in tibial diaphyseal fractures. *J Bone Joint Surg Br*. 1996;78:95–98.
53. Balogh Z, McKinley BA, Cox CS, Jr, et al. Abdominal compartment syndrome: the cause or effect of postinjury multiple organ failure. *Shock*. 2003;20:483–492.
54. Schubert AG. Exertional compartment syndrome: review of the literature and proposed rehabilitation guidelines following surgical release. *Int J Sports Phys Ther*. 2011;6:126–141.